Synthesis, structural characterization and anticancer activity of 3-(3,5-dinitrobenzoyl)-1*H*-imidazolidine-2-thione

Murat Genç[a], Özlem Keskin[a], Zübeyde Kumbıçak*[b], Özgür Vatan[c], Huzeyfe Huriyet[c] & Tolga Çavaş[c]

[a] Department of Chemistry, Faculty of Arts and Sciences, Adıyaman University, 02040, Adıyaman, Turkey

[b] Department of Molecular Biology and Genetics, Faculty of Arts and Sciences, Nevşehir Hacı Bektaş Veli University, 50300, Nevşehir, Turkey

[c] Department of Biology, Faculty of Arts and Sciences, Uludag University, 16059, Bursa, Turkey

E-mail: zkumbicak@nevsehir.edu.tr

The present study describes the synthesis, characterization and *in vitro* anticancer potential evaluation of a novel 3-(3,5-dinitrobenzoyl)-1*H*-imidazolidine-2-thione compound. In the first step, structure analysis of the compound has been elucidated by NMR and FT-IR techniques. Theoretical NMR, FT-IR spectra, HOMO and LUMO orbital energies and MEP analyses have been used to determine the activity of the molecule by Gaussian 09 package program using DFT techniques. Furthermore, docking calculations have been performed for the BRCA2 (PDB Code: 3EU7) active side to foresee the possible mechanism of action of the synthesized compound. In the second step of the study, the synthesized compound has been screened for its potential *in vitro* anticancer activity against MCF-7 human breast cancer cell line using the cell proliferation (XTT), apoptosis, cell cycle arrest and intracellular ROS production assays. The results of XTT test revealed significant dereases in MCF-7 cell viability with the 24h IC_{50} value of 7.57 μM. It has been also observed that treatment with the IC_{50} concentration of the compound can significantly induce apoptosis, intracellular ROS production and G2/M phase arrest in MCF-7 cells.

Keywords: Imidazole, BRCA2, AutodockVina, cytotoxicity, anticancer, MCF-7

Cancer is a disease characterized by the presence of gene products derived from genes that are mutated or abnormally expressed at somatic cell level. The combined effect of a large number of abnormal gene products leads to uncontrolled growth and spread in cancer cells. Some mutated cancer genes are hereditary, but they occur in most somatic cells. BRCA1 and BRCA2 genes are tumor suppressor genes and are known as breast cancer susceptibility genes and mutations in these genes are known to cause cancer. The BRCA1 gene has 24 exons and is located in the chromosome 17q21 and encodes a protein of 1863 amino acids. BRCA1 plays an important role in DNA repair, transcriptional regulation and control of cell growth. The BRCA2 gene consists of 27 exons and is located on the chromosome 12q13.2 and encodes a protein of 3418 amino acids. The BRCA2 is a nuclear protein expressed in the late-G1/early-S phase of the cell cycle[1]. BRCA2 is also described as a breast/ovarian cancer susceptibility gene by liaison analysis and until now approximately 2000 different BRCA2 mutations, variants or polymorphisms have been summarized in Breast Cancer Information Core (BIC). The proteins encoded by these genes are involved in homologous recombination and repair of double strand fractures lead to the development of one of the most common cancers in women[2].

Breast cancer gene expression profiles are named as complex and heterogeneous disease due to their different clinical status in the histological typing, lymph node status, invasion and metastasis and the breast cancer is considered one of the important diseases responsible for deaths worldwide. Currently, a variety of drugs are used in breast cancer chemotherapy. Imidazole is considered as an important agent in development of new drugs for

---

Abbreviations: BIC: Breast Cancer Information Core; MCF-7: Human breast cancer cell line; DFT: Density functional theory; PED: Potential energy distribution; HOMO: Highest occupied molecular orbital; LUMO: Lowest unoccupied molecular orbital; MEP: Molecular electostatic potential; FMO: Frontier molecular orbitals; VEDA: Vibrational energy distribution analysis; GIAO: Gauge-included atomic orbital; XTT: 2,3-Bis-(2-Methoxy-4-Nitro-5-Sulfophenyl)-2*H*-Tetrazolium-5-Carboxanilide) Cell Viability kit.

cancer treatment due to its heterocyclic ring containing a nitrogen atom of biological and pharmaceutical importance, therefore imidazole derivatives have played an important application in the treatment of cancer and an important agent used in medical chemistry[3].

Density functional theory (DFT) is widely used in theoretical modelling to characterize the molecules and can perform accurate calculations in reproducing experimental values in geometry, dipole moment and vibration frequency[4]. Docking is a method of predicting the orientation of a molecule to a second molecule when they are linked together to form a stable complex. It is used to estimate the affinity of small molecule drug candidates against protein targets, their binding to these proteins and therefore their biological activity[5,6]. Furthermore, in docking studies, the three-dimensional structure of the receptor binding energies can be determined and the position of the ligand at the receptor's binding region can be revived. This may be useful for understanding the type of binding and designing more compatible small-molecule ligands that target proteins[7,8]. On the other hand, synthesis of all new chemical compounds requires toxicity screening prior to drug design and development process. Therefore, it is essential to perform to demonstrate potential toxicity candidate compounds using different parameters such as cell viability, cell death mode, oxidative stress and cell cycle kinetics.

The aims of the present study were (I) to synthesize an imidazolidin-derived compound, (II) to obtain molecular structures of the compound using DFT, (III) to theoretically determine its docking profile and (IV) to evaluate possible *in vitro* cytotoxic activity of the compound using the xtt cell viability test, apoptosis, cell cycle arrest and intracellular Reactive Oxygen Species (ROS) production assays on a widely used model breast cancer cell line MCF-7.

Result and Discussion

Theoretical results

Optimized structure of the compound along with numbering of atoms was given in Figure 1.

FT-IR spectral analysis

The representative Fourier Transformed Infrared (FT-IR) spectrum of 3-(3,5-dinitrobenzoyl)-*1H*-imidazolidine-2-thione is illustrated in the Figure S1. Frequences of computed and experimental, potential

energy distribution (PED) of this molecule are summarized in Table S1. The aromatic C-H stretching bands of the compound was observed at 3220-3129 cm^{-1} in the FT-IR spectra and calculated as 3219-3131 cm^{-1}. In the literature[9], aromatic C-H vibrations were appeared in the range of 3100-3000 cm^{-1}. An intense IR absorption peak at 1671 cm^{-1} corresponded to the stretching vibrational mode of the C=O group of the title compound and calculated at 1771 cm^{-1}. As expected alphatic C-H vibrational peaks were observed at 2926-2881 cm^{-1}. In the FT-IR spectrum and calculated at 3096-3007 cm^{-1}, respectively. C-N stretching vibrations[10] have been appeared at 1246 cm^{-1}. For this study, this band is observed at 1623 cm^{-1} in FT-IR spectrum while the theoretical vibration is appeared of 1500 cm^{-1}.

In this study, aromatic C=C vibration are observed at 1458 cm^{-1} in FT-IR spectrum. Theoretical C=C stretching vibrations are calculated within the expected range. Because C=C vibrations are expected[11,12] to be found between 1300 and 1000 cm^{-1}. C=S strectching bandwith medium intensity was appeared at 1025–1225 cm^{-1} in FT-IR which is in accordance with the theoretical value of 536 cm^{-1}. It was also in good agreement with literature.

Nuclear Magnetic Resonance (NMR) spectral analysis

The experimental and theoretical ^{1}H and ^{13}C NMR are illustrated in Figure S2 and FigureS3, respectively. The GIAO, ^{1}H and ^{13}C NMR (with
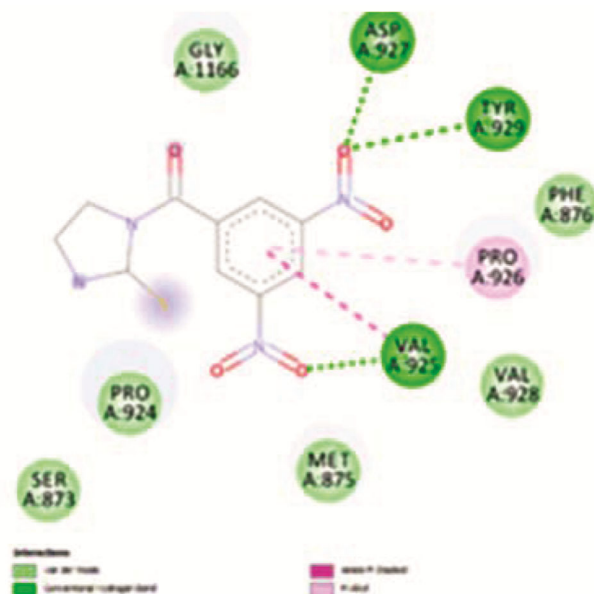
Figure 1 — Optimized structure of the compound

respect to TMS) of the compound were calculated in N,N-dimethyl sulfoxide (DMSO-d$_6$) B3LYP/6-311G+(d,p) method which are compared with experimental ^{1}H and ^{13}C chemical shift. The aromatic C-H protons appeared at δ 9.37-9.19 while this signal is computed at δ 8.90-8.70. The experimental chemical shift value for aliphatic C-H at δ 365-420 and δ 3.63-3.96 for theoretical.

The calculated chemical shift value δ 10.07 demonstrates the N-H protons in the molecule, while δ 10.37 in experimental N-H protons.

The ^{13}C NMR spectrum, carbonyl carbon peaks were appeared the experimentally were the region δ 165.78 where as the theoretical chemical shift values were computed at δ 175.80. The calculated aliphatic region chemical values were obtained at δ 54.28-56.03, where as they were δ 41.25-47.26 for experimentally determined ^{13}C NMR values. The C=S carbon in the 178.70 ring shows at δ 191.87. The other ^{1}H and ^{13}C NMR chemical shifts are summarized in Table S1, Table S2 and Table S3. The results showed that ^{1}H and ^{13}C chemical shifts are generally adjacent to the calculated ^{1}H and ^{13}C shift data.

Molecular electrostatic potential (MEP)

MEP is very useful in relation predicting molecule's electron density nucleophilic reaction and reactive charge of electrophilic to investigation of intermolecular hydrogen bonding interaction for biological identification. MEP is generally used to analyze the enzyme-substrate with drug –receptor inreractions and to investigate the processes the in compliance with identification in the region of the molecule.

The red regions observed after the MEP analysis indicate the maximum negative charge and for the compound these regions are S and O. The blue areas represent a positive charge, while the yellow and green areas represent negative and moderate negative charges. Imidazoline protons are blue color aromatic ring region in green color (Figure 2).

Frontier molecular orbitals (FMOs)

FMO play an important role in optical, electronic properties, chemical reactivity, kinetic stability and chemical conductivity of the compounds. Generally, a small FMO gap means the high chemical reactivity with a low kinetic stability which is called as a soft molecule[13]. The energy levels and distributions

energy levels of the highest occupied molecular orbital (HOMO), lowest unoccupied molecular orbital (LUMO), HOMO-1, LUMO+1 were computed at B3LYP/6-311G+(d,p) level for the compound. The energy level of HOMO and LUMO is -6.50461 eV and -3.45693 eV, respectively and the energy difference between HOMO and LUMO orbitals is 3.04768 eV. HOMO–1–LUMO+1 energy gap (ΔE) is -3.56795 (Figure 3).

Molecular docking

AutodockVina is used for the molecular docking studies to comment the nature of desired protein-ligand binding side and binding affinity. The high resolution crystal structure of tumor repressive in breast cancer (MCF-7) is used for molecular docking. The co-factors, ligand and water molecules in the target structure were taken out and additionally polar hydrogen atoms were inserted, after this stage selected torsion tree root and rotatable bonds were specified. Discover studio visualizer 3.5 (DSV 3.5)
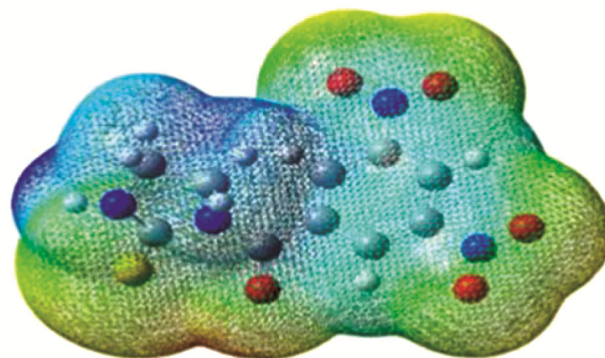

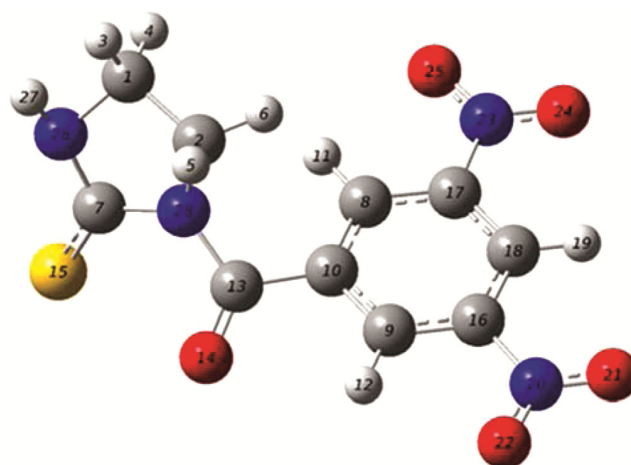Figure 2 — Molecular electrostatic potential map of the compound

Figure 3 — The frontier molecular orbitals of the compound

software was used to prepare both ligand and target structure[14]. In terms of the docking results illustrated in Figure 4, their interaction amino acids were attained as ASP 927 (with NO2's- O atom), TYR 929 (with NO2's- O atom), VAL 925 (with NO2's- O atom) and three hydrogen bonds.

Toxicity test results

Cell viability test

XTT assay was used to determine the cytotoxic effects of the compound and showed that the compound's induced dose-dependent manner. According to the results of the dose-response curve 50% inhibitory concentration (IC_{50}) compound, the average IC_{50} value was determined as IC_{50}=7.57 µM (p<0.005) (Figure 5).

Apoptotic assay

The degree of apoptosis in a cell population is an important parameter of cell health and is characterized by distinct morphological changes. Muse® Annexin V & Dead Cell Assay is based on the detection of phosphatidylserine on the surface of apoptotic cells[15]. The results on the apoptotic effects of the compound on MCF-7 cells were compared with negative and positive control groups (Figure 6). 7.57 µM (IC_{50} dose) of the compound was treated to the MCF-7 cells. The results showed that the treatment with 7.57
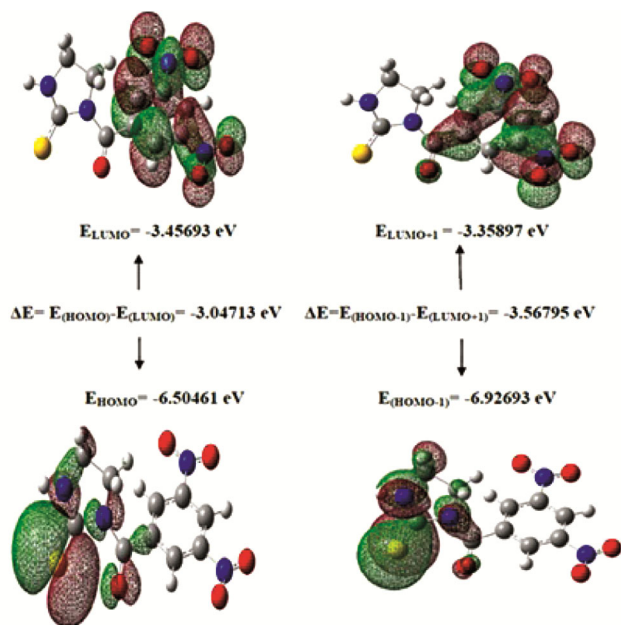
µM of the compound in MCF-7 cells, the rate of early and late apoptosis was 9.10% and 74.02%, respectively. For positive control group, the rate of early apoptosis was 11.62% and the late apoptosis was 8. 42%. The rates of early and late apoptosis were obtained in negative control group as 5.38% and 4.14%, respectively (Figure 7). Considering the results for negative and positive groups and compound, it has been found that the compound effects especially late apoptosis in MCF-7 cells.

Cell cycle assay

Cell cycle assay provides rapid and quantitative measurements of percentage of cells in the G0/G1, S, and G2/M phases of cell cycle. The percentage of cells in G0/G1, S and G2/M phases was calculated for negative and positive control groups and compound using by Muse Cell Analyzer. In the negative control group, the amounts of cells were obtained 60.6% in G0/G1, 13.3 % in Sand 25.9% in G2/M phases. In the positive control group, the amounts of cells were

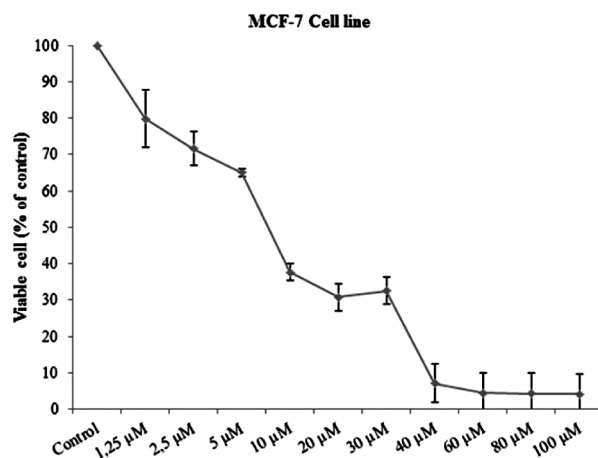Figure 5 — Viability of MCF-7 cells treated with the compound for 24 h by XTT assay

E_{LUMO}= -3.45693 eV E_{LUMO+1} = -3.35897 eV

$\Delta E= E_{(HOMO)}-E_{(LUMO)}$= -3.04713 eV $\Delta E=E_{(HOMO-1)}-E_{(LUMO+1)}$= -3.56795 eV

E_{HOMO} = -6.50461 eV $E_{(HOMO-1)}$= -6.92693 eV

Figure 4 — Themoleculardocking of thecompoundwith 3EU7 protein, showingsurfacerepresentationaroundligand (a) and 2D interactionplot of ligandwiththetarget (b)
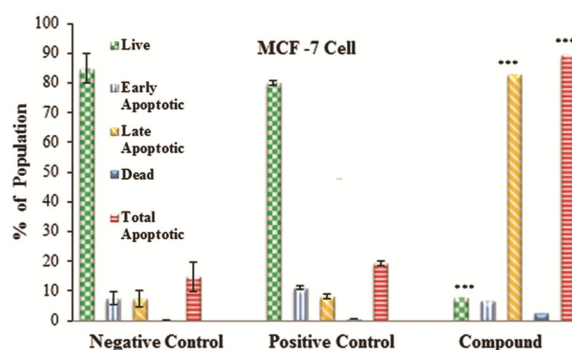
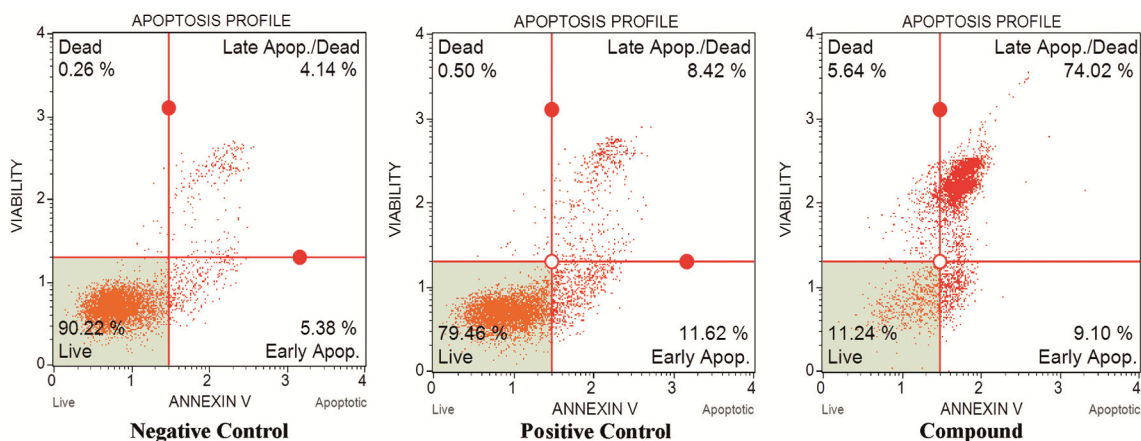Figure 6 — Histogram of apoptotic assay on MCF-7 cells (***p<0.005)

Figure 7 — Apoptotic effects of the compound on MCF-7 cells by Muse Annexin V and Dead Cell Assay compared with negative and positive control groups

determined 31.5% in G0/G1 ($p < 0.005$), 6.4 % in S ($p < 0.005$) and 61.4% in G2/M phases ($p < 0.005$). Finally, ratio of cells treated with the compound in G0/G1, S and G2/M phases were recorded as 56.6% ($p < 0.05$), 7.6% ($p < 0.001$) and 35.1% ($p < 0.001$), respectively. When the results were evaluated, the number of cells in the S phase was the lowest for all three groups. Cell ratios in G0/G1 phase were compared between the groups and it has shown that the positive group contains the lowest number of cells (31.5%) than the compound treated cells (56.6%). In the G2/M phase, the ratio of positive group cells (61.4%) were more than the compound cells (35.1%), but the negative control group cells were the lowest in the assay (Figure 8).

ROS assay

ROS assay assures the quantitative measurements of superoxide radicals in cells undergoing oxidative stress. MCF-7 cells were treated with 7.57 μM (IC$_{50}$ value) of compound to determine whether the compound causes ROS formation in MCF-7 cells. The results showed that a significant increase in intracellular ROS formation in MCF-7 cells when compared to the control groups and this data indicated that the compound raises the accumulation of intracellular ROS in MCF-7 cells ($p < 0.005$). Also, there was an increase of intracellular ROS in positive control group according to the negative control group, but this amount was lower than compound treated cells (Figure 9).

Heterocyclic compounds form the largest group of organic compounds[16]. Imidazole compounds play an important role in the pharmaceutical industry due to
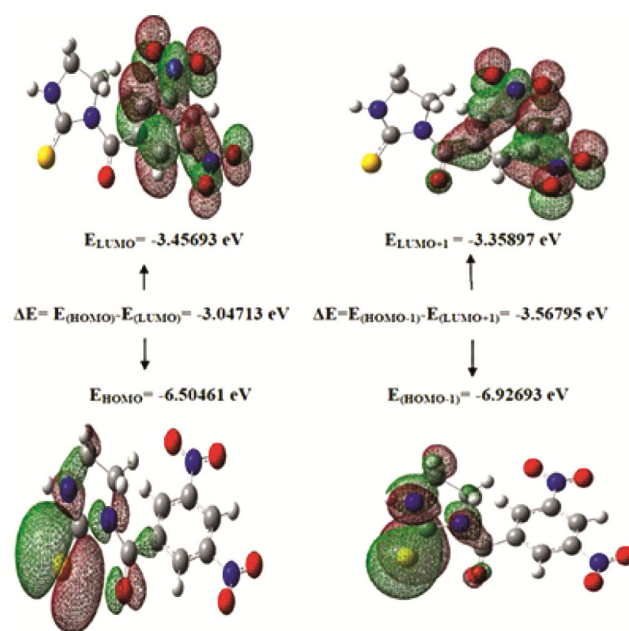

Figure 8 — The effect of compound on cell cycle in MCF-7 cells using Muse™Cell Cycle Reagent compared with negative and positive control groups

their antifungal, antimicrobial, anti-inflammatory, anticancer, antiviral, and antidiabetic properties. In the recent years, considerable efforts have been put into clinical, pharmacological and chemical characterization of novel imidazole-containing compounds for drug research and discovery[17]. Upto now, investigators have used many imidazolidine derivatives having imidazole rings for treatment on many different cancer types. For instance, Ghosh *et al.*[18] synthesized a new compound β-Tethymustine and demonstrated its *in vivo* curative effect in Swiss male mice against three murine ascites tumors namely
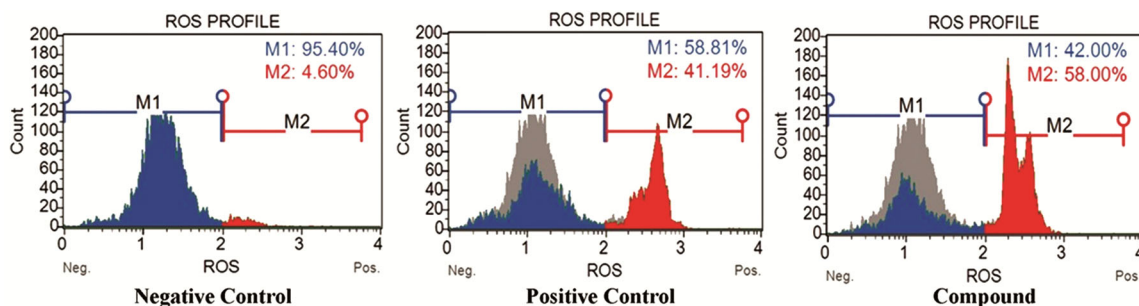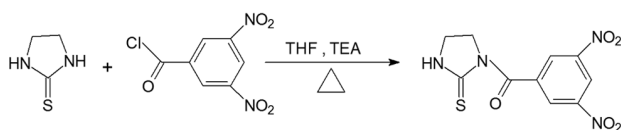
Figure 9 — Effect of the compound on intracellular ROS formation in MCF-7 cells

Scheme I — Synthesis of the compound

Ehrlich ascites carcinoma, sarcoma and Dalton's lymphoma. Similarly, Bolognese *et al.*[19] synthesized imidazoline containing quinolinquinone derivatives and demonstrated their antiproliferative activity against solid human tumor cells and reported that they are non intercalating DNA agents which inhibit the catalytic activitiy of topoisomerase II. Further studies have also demonstrated the antiproliferative effects of imidazolidin derivatives in various types of cancer cells such as leukemia, melanoma, non-small cell lung, lung, renal, ovarian, murine osteosarcoma and prostate[20-24]. These studies show that the imidazolidine derivatives are effective on many types of cancer, and emphasize the importance of investigation of their mechanism of action in cancer cells. In our study, the results of molecular docking analysis revealed an interaction between the compound and 3EU7 (crystal structure of BRCA2 complex) protein. This finding indicates that the mechanism of the action of the compound may also be related to the activity on RAD51 protein as the interaction of highly conserved BRC repeats (BRC1-4, BRC7, and BRC8) between BRCA2 and RAD51 proteins has been shown in numerous studies[25-28].

In normal cells, the RAD51 protein has many biochemical activities including homologous recombination and the ability to promote DNA chain exchange between homologous DNA molecules required for homologous recombination and DNA repair. As a precondition for these activities, RAD51 was incorporated into a protein sheath of DNA, it binds to DNA to form high-grade nucleoprotein filaments[29-31]. However, RAD51 protein is highly expressed in many human cancers types including breast, bladder, prostate, pancreas, soft tissue sarcoma, upper aerodigestive and lung cancer. This higher expression produces 840 times more transcribed products in cancer cells than in normal cells when the RAD51 promoter is activated. Furthermore, in clinical trials, patients with strong expression of RAD51 were found to have more aggressive pathological features and negative results than expected[32]. In this case, BRCA2 is important for RAD51 function and has become a new target to overcome the various cancer types especially breast cancer[4].

Many anticancer drugs provide cell death by creating DNA damage. In this case, DNA repair pathways create resistance to the drug. Therefore, inhibition of enzymes that repair DNA is one of the main goals of cancer treatment[33]. According to our results, we suggest that our compound acts as a BRCA2 inhibitor to induce interaction with RAD51 by binding to BRCA2 at three types of amino acids (Aspartic acid, Tyrosine, Valine) and three hydrogen bonds. Thus, blocking BRCA2 may also limit the effectiveness of RAD51. Furthermore, in our study, the results of cell cycle analysis showed that the proportions of cells in the S phase were 13.3% and 7.6% in negative control and treatment groups, respectively, which indicates possible reduction in DNA synthesis in MCF-7 Cells.

In our toxicity tests, the compound appeared to increase the intracellular ROS formation in comparison with negative control which may lead to cell death by apoptosis. In fact, the increase in ROS can be attributed to reasons such as DNA degradation, DNA oxidation, and depletion of decreased glutathione. For this reason, it is very important that the damaged cells can be eliminated by apoptosis pathway.

Experimental Section
Materials

All chemicals used in this study were of analytical grade and were used without any further purification.

Instruments

Structure analysis of the compound was elucidated experimentally by NMR (using Bruker 300 MHz Spectrometer, Inonu University, Malatya) and FT-IR (using Perkin Elmer Spectrometer, Adıyaman University, Adıyaman) methods.

Synthesis of the 3-(3,5-dinitrobenzoyl)-*1H*-imidazolidine-2-thione

50 mL 0.01 mol (1.02 g) of imidazolidin-2-thione, 0.03 mol of triethylamine and 20 mL of tetrahydrofuran were added to the test flask and stirred at room temperature for 20 min. 3,5-Dinitrobenzoylchloride was added to the reaction medium. The reaction was continued for 24 h at the boiling temperature of the solvent, increasing the temperature controlled under reflux. The mixture was filtered hot. Solvent was removed in the rotary evaporator under vacuum. The crude product was crystallized from ethyl alcohol (Scheme I).

Chemical formula was $C_{19}H_8N_4O_5S$ (Yield 75%) and molecular weight was 296.26. Melting point was 216.7°C. FT-IR (ATR): 3220–3129 (aromatic C-H stretching), 2926-2881 (aliphatic C-H stretching), 1671 (C=O stretching), 1623 (C-N stretching), 1458 (aromatic C=C stretching), 718 cm^{-1} (C=S bending) (Figure S1); ^{1}H NMR (300 MHz, DMSO-d_6): δ 3.36 (J = 6Hz, H_2, 2H), 4.19 (J = 6H$_z$, H_1, 2H), 8.74 ($H_{8,9}$, 2H), 8.91 (H_{18}, 1H), 10.07 (H_{26}, 1H) (Figure S2); ^{13}C NMR (300 MHz, DMSO-d_6): δ 41.25 (C-1), 47.26 (C-2), 119.81 (C-18), 128.07 (C-8), 138.96 (C-9, C-10), 146.93 (C-16 and C-17), 165.78 (C-13), 178.70 (C-7) (Figure S3).

Computational Details

GAUSSIAN 09 program was used for DFT/B3LYP with 6-311G+(d,p) basis set[34,35]. For this study, Becke three parameters hybrids functional method which consist of non-local swap functional of Becke style and Lee, Yang, Parr's non-local correlation functional were used[36,37]. Geometrical parameters and vibrational assigment were calculated to obtain optimization of the geometry. Thereafter, the vibrational energy distribution analysis (VEDA) was used to get PED analysis[38]. In order to confirm MEP were computed for the compound. ^{1}H NMR and ^{13}C NMR chemical shift were calculated by employing the gauge-included atomic orbital (GIAO) approach.

Molecular Docking Studies

So as to get a molecular interaction profile of imidazoline derivatives as antitumor agents, the crystal structure of BRCA2 was attained from the protein data bank (PDB Code: 3EU7) and used for arrangement and docking of the structure synthesized. The computed of the docking energies of the ligand inside the BRCA2 active side was applied using the software AutodockVina program. The results of docking were visualized by Discovery Studio 3.5 program.

Toxicity test methods

Cell culture

MCF-7 cell line were purchased from American Type Culture Collection (ATCC). Cells were maintained in Roswell Park Memorial Institute (RPMI) 1640 Medium supplemented with 10% fetal bovine serum (FBS), 2 mM L-glutamine, penicillin-streptomycin (50 µg/mL). Cells were cultured in an incubator containing a humidified atmosphere of 5% CO_2 in air and maintained at 37 °C.

Cell viability test

Potential effects of the compound on viability of MCF-7 cells were determined using XTT assay. Cell viability by XTT is based on enzyme's mitochondrial activity on living cells, which become inactive just after cell death. Growing MCF-7 cells (1×10^5 cells/mL) were seeded on to 96 well plate and treated with serial concentrations of compound (1.25, 2.5, 5, 10, 20, 30, 40, 60, 80 and 100 µM) for 24 h. 200 µL phosphate buffered saline (PBS) was washed to each well. Then 100 µL RPMI 1640 medium and 50 µL Activated-XTT solutions were added to each well. The plate was incubated for 4 h at 37°C. Absorbance was read at 450 nm and 630 nm by a microplate reader (Biotek elx800).The percent viability of cells was calculated as follows:

$$\text{Viability \%} = 100 \times (A_{\text{experiment groups}} / A_{\text{control groups}})$$

Apoptotic assay

Muse® Annexin V &Dead Cell Assay Kit were used to investigate cell death pathway. MCF-7 cells were seeded in T25 flask (4×10^4 cells) in 3 mL RPMI. After cells were treated with IC_{50} dose of compound in 24 h. Cells were centrifuged at 300 g for 5 min and washed with 1× PBS and were incubated in 100 µl of Muse®Annexin V & Dead Cell reagent for 20 min before being analyzed by Muse Cell Analyzer.

Cell cycle assay

Muse® Cell Cycle Assay Kit was used to determine quantitative measurements of the

percentage of cells in the G0/G1, S or G2/M phases of cell cycle. MCF-7 cells were seeded in T25 flask (4×10^4 cells) in 3 mL RPMI. After cells were treated with IC_{50} dose of compound in 24 h. Cells were collected 1×10^6 per tube. Tubes were centrifuged 300 g for 5 min and washed with $1 \times$PBS. Pellets were fixed in cold %70 ethanol. MCF-7 cells were kept in -20 °C at least 3 h. After centrifugation of the cells at 300 g for 5 min, the cells were washed once with $1 \times$ PBS. Then 200 µL of Muse™Cell Cycle Reagent was added to each tube, incubated for 30 min at room temperature. Cells were analyzed by Muse® Cell Analyzer (Millipore) at the end of process.

ROS assay

Muse® Oxidative Stress Assay Kit was used to obtain quantitative measurements of ROS, namely superoxide radicals in cells undergoing oxidative stress. MCF-7 cells were seeded in T75 flask (5×10^6 cells) in 10 mL RPMI. After, cells were treated with IC_{50} dose of compound in 24 h. Cells were harvested $1 \times 10^6 - 1 \times 10^7$ per tube and assay was performed according to the protocol of the Muse® Oxidative Stress Assay Kit.

Experiments were repeated for three times and IC_{50} dose of Colchicine was used for positive control groups.

Statistical analysis

Statistical analysis was actualized by SPSS Version 21.0. Data were revealed as percent of control of mean ± SD by one-way analysis of variance, ANOVA followed by the Tukey test. $p < 0.005$ and $p < 0.001$ were considered as the level of significance for value obtained for test groups and compared with the negative groups.

Conclusions

In addition to the determined cytotoxic effects of compound, the molecular structure, arrangement of atoms, presence of nitrogen atoms, ring geometry could also be important elements of its anticancer activity. Based on the results of our preliminary study with the synthesized compound, further investigations of imidazolidine derivatives, DNA interactions, and their effects on different cancer cells will be carried out.

Supplementary Information

Supplementary information is available in the website http://nopr.niscair.res.in/handle/123456789/58776.

Acknowledgements

References

1   Monguaoğlu A E, Lüleci G, Özçelik T, Çolak T, Schayek H, Akaydın M &FriedmanE, *Hum Mutat*,21 (2003) 444. DOI: 10.1002/humu.9119
2   Cooper G M, *The Cell*: *A Molecular Approach* (The American Society for Microbiology, Washington, USA) (1997).
3   Baroniya S, Anwer Z, Sharma P K, Dudhe R & Kumar N, *Der Pharmacia Sinica*, 1(2010) 172.
4   Genç Z K, Tekin S, Sandal S, Sekerci M &Genç M, *Res ChemIntermed*, 41 (2014) 4477. DOI: 10.1007/s11164-014-1545-5
5   Kitchen D B, Decornez H, Furr J R &Bajorath J, *Nat Rev Drug Discov*, 3 (2004) 935. DOI: 10.1038/nrd1549
6   Chikhi A &Bensegueni A, *Journal of Proteomics & Bioinformatics*, 1 (2008) 161. DOI:10.4172/jpb.1000022
7   Holt P A, Chaires J B & Trent J O, *J ChemInf Model*, 48 (2008) 1602. DOI: 10.1021/ci800063v
8   Öztürk Ö, *DissertationAnkara University* (2013).
9   Upadhyaya P & Devi Th G, *VibSpectrosc*, 96 (2018). DOI:10.1016/j.vibspec.2018.03.006
10 Puviarasan N, Arjunan V & Mohan S, *Turk J Chem*, 26 (2002) 323.
11 Bellamy L J, *The Infrared Spectra of Complex Molecules* (John Wiley, New York) (1959).
12 Varsanyi G, *Vibrational Spectra of Seven Hundred Benzene Derivatives* (Academic Press, New York) (1969).
13 Yilmaz E, *Journal of Molecular Strucutre*, 1166 (2018) 407. DOI: 10.1016/j.molstruc.2018.04.060
14 Yilmaz E &Cukurovali A, *Canadian J Physics*, 97 (2019) 408. DOI: 10.1139/cjp-2018-0302
15 Khan A, Gillis K, Clor J &Tyagarajan K, *Postepybiochemii*, 58 (2012) 492.
16 Hart H, Hart D J &Craine L E, *OrganikKimya*, (Çev: Uyar T), *Palme Yayıncılık*, Ankara (1998).
17 Üstün Z, *DissertationSüleymanDemirel University* (2018).
18 Ghosh M, Bhattacharya S, Sadhu U, Dutta S &Sanyal U, *Cancer Lett*, 119(1) (1997) 7. DOI: 10.1016/s0304-3835(97)00244-9
19 Bolognese A, Correale G, Manfra M, Esposito A, Novellino E &Lavecchia A, *J Med Chem*, 51 (2008) 8148. DOI: 10.1021/jm8007689
20 BasappaAnanda Kumar C S, NanjundaSwamy S, Sugahara K &Rangappa K S, *Bioorg Med Chem*, 17 (2009) 4928. DOI: 10.1016/j.bmc.2009.06.004
21 Cesarini S, Spallarossa A, Ranise A, Schenone S, Rosano C, La Colla P, Sanna G, Busonera B &Loddo R, *Eur J Med Chem*, 44 (2009) 1106. DOI: 10.1016/j.ejmech.2008.06.010

22 MukherjeeA, DuttaS, ChashooG, BhagatM, SaxenaA K & SanyalU, *Oncol Res*, 17 (2009) 387. DOI: 10.3727/096504009788912516

23 Thirupathi R Y, Narsimha R P, Koduru S, Damodaran C & Crooks P A, *Bioorg Med Chem*, 18 (2010) 3570. DOI: 10.1016/j.bmc.2010.03.054

24 ShahA, Nosheen E, Munir S, Badshah A,Qureshi R, Rehman Z, Muhammad N &Hussain H, *J PhotochemPhotobiol B*, 120 (2013) 90. DOI: 10.1016/j.jphotobiol.2012.12.015

25 Mizuta R, LaSalle J M, Cheng H L, Shinohara A, Ogawa H, Copeland N, Jenkins N A, Lalande M & Alt F W, *PNAS* (*USA*), 94 (1997) 6927. DOI: 10.1073/pnas.94.13.6927

26 Wong A K, Pero R, Ormonde P A, Tavtigian S V & Bartel P L, *J BiolChem*, 272 (1997) 31941. DOI: 10.1074/jbc.272.51.31941

27 Chen P L, Chen C F, Chen Y, Xiao J, Sharp Z D & Lee W H, *PNAS* (*USA*), 95 (1998) 5287. DOI: 10.1073/pnas.95.9.5287

28 Marmorstein L Y, Ouchi T & Aaronson S A, *PNAS* (*USA*), 95 (1998) 13869. DOI: 10.1073/pnas.95.23.13869

29 Benson F E, Stasiak A & West S C, *EMBOJ*, 13 (1994) 5764.

30 Davies A A, Masson J Y, Mcllwraith M J, Stasiak A Z, Stasiak A, Venkitaraman A R & West S C, *Molecular Cell*, 7 (2001) 273. DOI: 10.1016/s1097-2765(01)00175-7

31 Mcllwraith M J, Van Dyck E, Masson J Y, Stasiak A Z, Stasiak A & West S C, *J MolBiol*, 304 (2000) 151. DOI: 10.1006/jmbi.2000.4180

32 Budke B, Logan H L, Kalin J H, Zelivianskaia A S, McGuire W C, Miller L L, Stark J M, Kozikowski A P, Bishop D K & Cornell P P, *Nucleic Acids Res*, 40 (2012) 7347. DOI: 10.1093/nar/gks353

33 Tok F & Koçyiğit-Kaymakçıoğlu B, *Müsbed*, 1 (2015) 41. DOI: 10.5455/musbed.20141015015238

34 Frisch M J, Trucks G W, Schlegel H B, Scuseria G E, Robb M A, Cheeseman J R, Scalmani G, Barone V, Mennucci B, Petersson G A, Nakatsuji H, Caricato M, Li X, Hratchian H P, Izmaylov A F, Bloino J, Zheng G, Sonnenberg J L, Hada M, Ehara M, Toyota K, Fukuda R, Hasegawa J, Ishida M, Nakajima T, Honda Y, Kitao O, Nakai H, Vreven T, Montgomery J A Jr, Peralta J E, Ogliaro F, Bearpark M J, Heyd J J, Brothers E N, Kudin K N, Staroverov V N, Kobayashi R, Normand J, Raghavachari K, Rendell A P, Burant J C, Iyengar S S, Tomasi J, Cossi M, Millam J M, Klene M, Knox J E, Cross J B, Bakken V, Adamo C, Jaramillo J, Gomperts R, Stratmann R E, Yazyev O, Austin A J, Cammi R, Pomelli C, Ochterski J W, Martin R L, Morokuma K, Zakrzewski V G, Voth G A, Salvador P, Dannenberg J J, Dapprich S, Daniels A D, Farkas Ö, Foresman J B, Ortiz J V, Cioslowski J & Fox D J, Gaussian 09, Gaussian, Inc., Wallingford CT. https://gaussian.com/glossary/g09/ (accessed: July 22, 2019).

35 Becke A D, *J ChemPhys*, 98 (1993) 5648. DOI: 10.1063/1.464913

36 Dennington R, Keith T &Millam J, GaussView Version 5 SemichemInc, Shawnee Mission KS, (2009).

37 Lee C, Yang W & Parr R G, *Phys Rev B Condens Matter*, 37 (1988) 785. DOI: 10.1103/physrevb.37.785

38 Michal H J, Vibrational Energy Distribution Analysis VEDA 4. https://www.smmg.pl/software (2004-2010).